

Tilted Brownian Ratchet for DNA Analysis

Lotien Richard Huang,[†] Edward C. Cox,[‡] Robert H. Austin,^{*,§} and James C. Sturm[†]

Center for Photonics and Optoelectronic Materials (POEM), Departments of Electrical Engineering, Molecular Biology, and Physics, Princeton University, Princeton, New Jersey 08544

In this paper, we report a factor of 3 improvement in the resolution and a factor of 10 improvement in the speed of fractionation of ~100-kb DNA molecules in Brownian ratchet arrays. In our device, the electrophoretic flow is tilted at a small angle relative to the array axis. Tilting accelerates the fractionation speed because a higher fraction of the diffusing molecules is “ratcheted” at each step in the array. Molecules of lengths 48.5 and 164 kb can be separated in ~70 min with a resolution of ~3.8, using a 12-mm-long array. The Brownian ratchet arrays are not limited to DNA separation, but can, in principle, be used for any particle in this size range.

The analysis and separation of DNA molecules larger than 40 000 base pairs plays a key role in many genome projects. Standard agarose gel electrophoresis is incapable of separating molecules larger than approximately 40 kb. Large DNA fragments are therefore separated by pulsed-field gel electrophoresis (PFGE), which is time-consuming, with running times of typically more than 10 h.¹

One class of novel approaches toward achieving higher separation speeds is based on microfluidics, where DNA fragments flow through microfabricated structures.² In one such approach, an entropic trap array consisting of many narrow gaps (<100 nm) separating regions of a 2- μ m-deep channel, molecules in the ~100-kb range can be separated in ~30 min.³ When narrower than the radius of gyration of the DNA molecules, these gaps act as entropic barriers that retard the motion of small molecules more than larger ones. In a second approach, a hexagonal array of micrometer-sized posts replaces the agarose gel in a conventional pulsed-field electrophoresis configuration. This reduces the running time to less than 1 min.⁴

A third microfluidic approach exploits Brownian ratchets, structures that permit Brownian motion in only one direction.^{5,6} This method works by driving particles through an array of

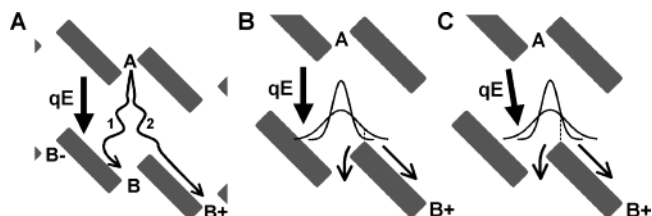


Figure 1. Basic principle of the Brownian ratchet array. Particles are driven through the array hydrodynamically or electrophoretically (pictured). (A) The rectangular obstacle array prevents particles emerging from gap A and diffusing to the left (1) from reaching gap B- but ratchets particles diffusing to the right (2) to gap B+. (B) Particles of different sizes diffuse to different extents (bell-shaped curves represent lateral distributions of small and large particles), resulting in different probabilities of deflection to B+. The vertical dotted line within the distributions represents the required diffusion for ratcheting to gap B+. (C) The probability of a particle being deflected to B+ is increased by tilting the flow at a small angle with respect to the vertical axis of the array.

micrometer-sized obstacles, each one tilted with respect to the flow.^{7,8} When particles flow through such an array (Figure 1A), particles diffusing to the left (path 1, Figure 1A) are blocked and deflected back to gap B, whereas those diffusing to the right (path 2) are deflected to gap B+. The probability of deflection depends on the diffusion coefficient of the particle (Figure 1B). Small molecules thus have a higher probability of being ratcheted than larger ones, and on average, the smaller molecules migrate at a greater angle with respect to the vertical axis. A major advantage of the Brownian ratchet array over the entropic trap array and the hexagonal post array is that the ratchet array does not require stretching of the molecules—globular molecules and molecules of other shapes can be sorted in the same run according only to their diffusion coefficients.⁹ However, the separation of large molecules in a microfabricated Brownian ratchet array is slow because it relies on diffusion,¹⁰ an intrinsically slow process. To date, this slow speed has limited the potential usefulness of the ratchet array.

Here, we report that the separation of large molecules can be improved dramatically by tilting the electrophoretic flow relative to the vertical axis of the array (Figure 1C). This improvement occurs because, for the same amount of diffusion, the probability that a molecule will be deflected is greatly increased compared

* To whom correspondence should be addressed. E-mail: austin@princeton.edu.

[†] Department of Electrical Engineering.

[‡] Department of Molecular Biology.

[§] Department of Physics.

(1) Sambrook, J.; Fritsch, E. F.; Maniatis, T. *Molecular Cloning: A Laboratory Manual*, 2nd ed.; Cold Spring Harbor Laboratory Press: Cold Spring Harbor, NY.

(2) Volkmuth, W. D.; Austin, R. H. *Nature* **1992**, *358*, 600–602.

(3) Han, J.; Craighead, H. G. *Science* **2000**, *288*, 1026–1029.

(4) Huang, L. R.; Tegenfeldt, J. O.; Kraeft, J. J.; Sturm, J. C.; Austin, R. H.; Cox, E. C. *Nat. Biotechnol.* **2002**, *20* (10), 1048–1051.

(5) Feynman, R. P.; Leighton, R. B.; Sands, M. *The Feynman Lectures on Physics*; Addison-Wesley: Reading, MA, 1966; Chapter 46, Vol. 1.

(6) Astumian, R. D. *Science* **1997**, *276*, 917–922.

(7) Duke, T. A. J.; Austin, R. H. *Phys. Rev. Lett.* **1998**, *80*, 1552–1555.

(8) Ertas, D. *Phys. Rev. Lett.* **1998**, *80*, 1548–1551.

(9) van Oudenaarden, A.; Boxer, S. G. *Science* **1999**, *285*, 1046–1048.

(10) Huang, L. R.; Silberzan, P.; Tegenfeldt, J. O.; Cox, E. C.; Sturm, J. C.; Austin, R. H.; Craighead H. *Phys. Rev. Lett.* **2002**, *89*, 178301–178304.

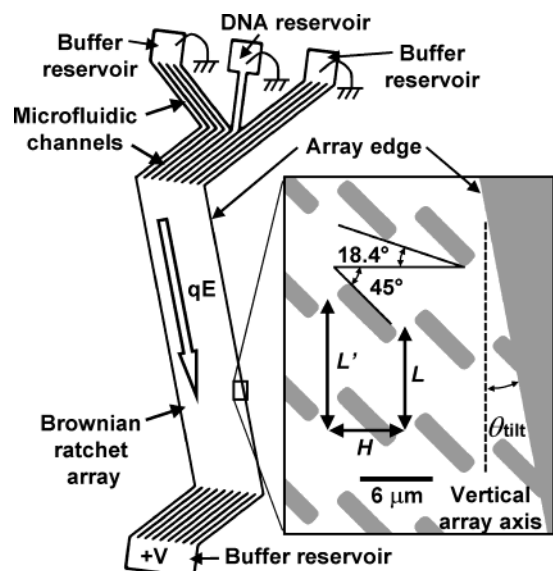


Figure 2. Schematic diagram of the device at the flow angle of $\theta_{\text{tilt}} = 10.8^\circ$ with respect to the vertical array axis. Devices with angles of $\theta_{\text{tilt}} = 0^\circ, 3.6^\circ,$ and 7.2° were identical except for θ_{tilt} . The pitch of the columns of obstacles, the vertical pitch of the rows, and the vertical distance from gap A to gap B+ (Figure 1A), defined as $H, L,$ and $L',$ respectively, were 6, 8, and 10 μm , respectively, in our experiments. The obstacles were $\sim 5.6 \mu\text{m}$ long, $\sim 1.4 \mu\text{m}$ wide, and $\sim 3.2 \mu\text{m}$ tall.

to the case where the flow is aligned along the vertical array axis, as it is in Figure 1A and B.¹⁰

EXPERIMENTAL SECTION

Ratchet Design. We used the same geometry of the obstacle array as in our previous work (Figure 2),^{7,10} where the individual obstacles and the obstacle rows are tilted at 45° and 18.4° , respectively, relative to the vertical array axis (Figure 2 inset). These two angles make the array asymmetric and are fundamental to the “ratcheting” behavior. The focus of this paper is not to optimize the array geometry, but rather to present flow tilting as a general method for effectively enhancing the performance of ratchets with a given array geometry. The direction of electrophoretic flow, carried by ions in the fluid, is tilted with respect to the vertical array axis by a small angle, θ_{tilt} . Individual arrays were made for θ_{tilt} values of $0^\circ, 10.3.6^\circ, 7.2^\circ,$ and 10.8° .

Generation of Tilted Flow. Because of the asymmetry in the array, the average direction of the ion flow is generally not perpendicular to the equipotential contours.¹⁰ Three features are incorporated in the device design to control the average current direction and create straight bands of molecules throughout the array (Figure 2): (i) The array is long and narrow (13 mm by 3 mm) and essentially one-dimensional, with flow lines parallel to the side edges. (ii) To create the correct boundary conditions at the top and bottom of the array, the top and bottom edges are slanted at an angle, chosen to set the edges along equipotential lines determined by numerically solving the Laplace equation for the array geometry for each value of θ_{tilt} .¹⁰ (iii) Microfluidic channels leading into the array act as electrical resistors, each one of which will carry approximately the same amount of current. The resistance of their parallel combination is large compared to the sheet resistance of the array. This reduces any residual distortion of the current distribution near the top and bottom edges.¹¹

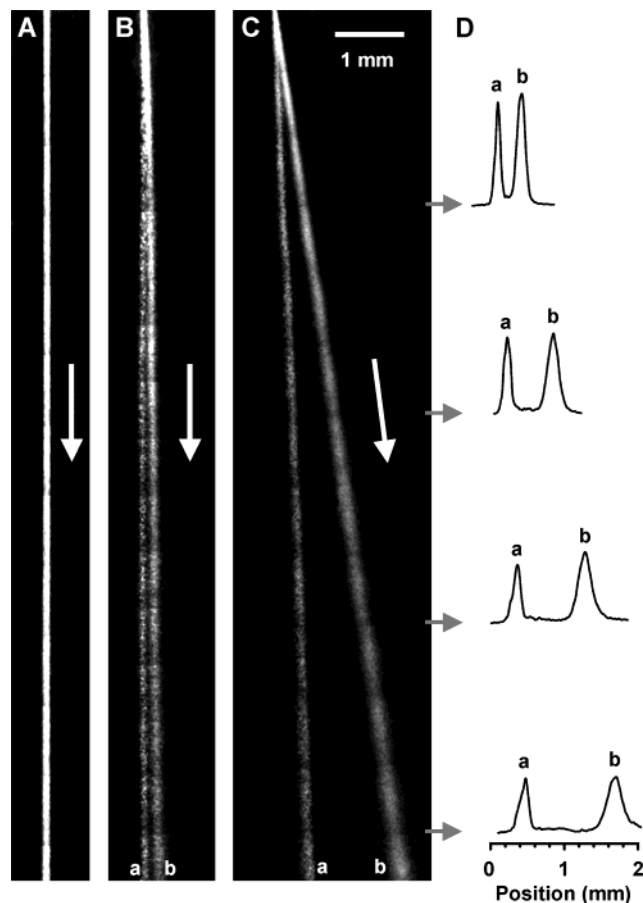


Figure 3. Fluorescent micrograph of 48.5- and 164-kb DNA in Brownian ratchet arrays. The molecules were injected at a single point at the top of the array and run at different flow conditions. The array axis is vertical in all micrographs. The arrow shows the direction of the ionic flow θ_{tilt} . (A) Zero flow tilt angle ($\theta_{\text{tilt}} = 0^\circ$) and high speed ($\sim 24 \mu\text{m/s}$). (B) Zero flow tilt angle ($\theta_{\text{tilt}} = 0^\circ$) and low speed ($\sim 1.5 \mu\text{m/s}$). Band assignment for DNA: (a) 164 kb, (b) 48.5 kb. (C) Tilted flow ($\theta_{\text{tilt}} = 7.2^\circ$) at $\sim 1.5 \mu\text{m/s}$. (D) Electrophoretograms of C measured 3, 6, 9, and 12 mm from the injection point.

The straight bands of DNA in Figure 3 demonstrate that this approach was successful.

Device Fabrication. Tilted ratchet arrays were fabricated using conventional photolithography and reactive-ion-etching techniques. Fused-silica wafers were chosen as substrates because DNA was to be electrophoresed through the arrays. The etched wafers were sealed with glass coverslips to form enclosed microfluidic channels. Samples were introduced into the channels through holes sand-blasted through the substrate wafer.

Electrophoresis Conditions. A mixture of coliphage λ and T2 DNA (48.5 and 164 kb, respectively) at concentrations of ~ 2 and $\sim 1 \mu\text{g/mL}$, respectively, was used as a test system and visualized by fluorescent microscopy. DNA was stained with TOTO-1 (Molecular Probes) at a ratio of 1 dye molecule per 10 base pairs. POP-6 (0.1%), a performance-optimized linear polyacrylamide (Perkin-Elmer Biosystems), and 10 mM dithiothreitol (DTT) were added to the $1/2 \times$ Tris–Borate–EDTA buffer to suppress electroosmotic flow and photobleaching, respectively. The flow speeds of the molecules were controlled by the voltage

(11) Huang, L. R.; Tegenfeldt, J. O.; Kraeft, J. J.; Sturm, J. C.; Austin, R. H.; Cox, E. C. *Tech. Dig.-Int. Electron Devices Meet.* **2001**, 363–366.

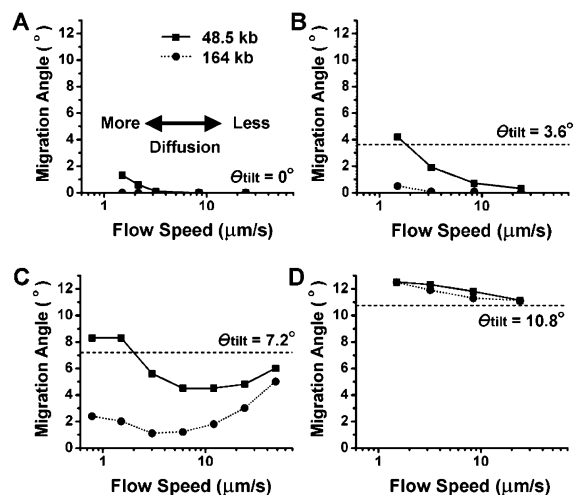


Figure 4. Measured migration angles of DNA molecules as functions of flow speed, at (A) zero ion flow angle ($\theta_{\text{tilt}} = 0^\circ$), (B) $\theta_{\text{tilt}} = 3.6^\circ$, (C) $\theta_{\text{tilt}} = 7.2^\circ$, and (D) $\theta_{\text{tilt}} = 10.8^\circ$. For comparison, the dotted horizontal lines show θ_{tilt} . Lower speed allows for more diffusion and more ratcheting.

applied to the reservoirs and measured by observing the velocities of individual molecules.

RESULTS AND DISCUSSION

When the ion flow direction was aligned to the array ($\theta_{\text{tilt}} = 0^\circ$), as in all previous work,¹⁰ with an applied voltage sufficient to drive the DNA at relatively high flow speeds ($>4 \mu\text{m/s}$), the two species of DNA migrated in the same direction at approximately the same speeds (Figure 3A). No separation occurred because of the insufficient time for molecules to diffuse over the distance required for ratcheting. When the speed was reduced to $\sim 1.5 \mu\text{m/s}$, which allowed for more diffusion, the 48.5-kb λ DNA migrated at an angle of $\sim 1.3^\circ$ relative to the 164-kb T2 DNA (Figure 3B). The identity of the bands was established by directly observing the molecules' size using a high-magnification ($60\times$) objective.¹⁰ At the end of the 12-mm array, the resolution of the two bands, defined as $\Delta X / (2\sigma_1 + 2\sigma_2)$ to measure the peak separation ΔX relative to the full bandwidths ($2\sigma_1$ and $2\sigma_2$), was ~ 1.4 .¹²

Figure 3C shows the results of the same type of experiment when the ion flow was applied at 7.2° with respect to the vertical array axis ($\theta_{\text{tilt}} = 7.2^\circ$, velocity $\approx 1.5 \mu\text{m/s}$). The deflection of the 48.5-kb DNA was greatly increased from the previous case, where $\theta_{\text{tilt}} = 0$, and even the 164-kb molecules were somewhat deflected from the vertical direction. This can be qualitatively understood from Figure 1C, which shows that the fraction of transversely diffusing molecules captured by the ratchet is increased by tilting the direction of ion flows. Most significantly, the separation angle (defined as the angle between the two bands) has now increased from 1.3° to 6.3° , and the resolution from ~ 1.4 to ~ 4.1 . Figure 3D shows the electrophoretograms under these conditions measured 3, 6, 9, and 12 mm from the top of the array.

The migration direction of a molecule with respect to the vertical array axis (defined as migration angle θ_{mig}) is plotted as a function of DNA flow speed for flow angles (θ_{tilt}) of 0° , 3.6° , 7.2° , and 10.8° in Figure 4. Also shown schematically (dotted lines) in each panel is the tilt angle of ion flow (θ_{tilt}) with respect to the vertical array axis. As expected, the migration angles at a tilt of

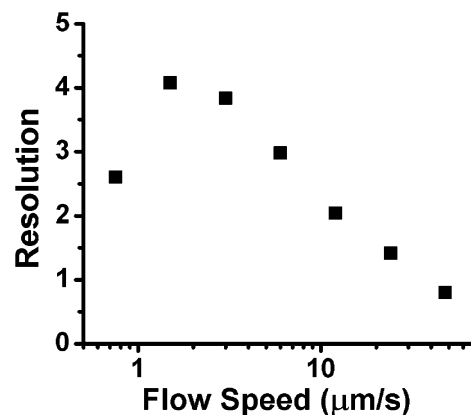


Figure 5. Resolution of 48.5- and 164-kb molecules at $\theta_{\text{tilt}} = 7.2^\circ$ and various flow speeds measured 12 mm from the injection point.

3.6° are greater than those for no tilt ($\theta_{\text{tilt}} = 0^\circ$), and they decrease at higher flow speeds, again because there is insufficient time for diffusion. At $\theta_{\text{tilt}} = 7.2^\circ$, the migration angles and separation are larger still, and the migration angles decrease as expected with flow speeds up to about $6 \mu\text{m/s}$. At larger speeds, surprisingly, they increase again. We believe that this is because DNA elongates and reptates at high fields, thus giving it a smaller cross section, so that it behaves like a smaller particle as it passes through the gaps. The DNA then is not subject to ratcheting, but follows the direction of ion flow.¹⁰ At a tilt of 10.8° , both large and small molecules migrate at similar large angles, independent of flow speeds, with little separation. We believe that this occurs because we are beginning to approach the critical tilt condition ($\sim 18^\circ$ in our case) at which half of the flow lines would be diverted to the adjacent gap solely by the tilt, independent of diffusion. This would lead to a breakdown of ratcheting. In any case, data for this array geometry show that the optimum angle θ_{tilt} for separation is $\sim 7^\circ$.

Figure 5 shows the dependence of resolution¹² on flow speed at $\theta_{\text{tilt}} = 7.2^\circ$. As expected, at high flow speeds, the resolution decreases because of insufficient time for diffusion. At very low speeds, however, resolution decreases again, this time because of excessive diffusion, leading to band broadening.

The rate of band broadening is important because it affects the resolution with which molecules of different sizes can be separated. Band broadening in a ratchet array should follow a binomial distribution,¹³ because the positions of molecules are reset to the centers of the gaps each time the molecules pass through the gaps.^{7,10} Therefore, each ratcheting event is statistically independent, and both the migration angle θ_{mig} and band broadening should depend on a single parameter, p , the probability of a molecule being deflected after one row of obstacles.^{7,8} According to the geometry of the array (Figure 2, inset), a molecule will shift a distance H horizontally and L' vertically if deflected, or a distance L if it is not deflected. Therefore, the average displacement after one row of obstacles is Hp horizontally and $L(1 - p) + L'p$ vertically; the average migration angle θ_{mig} is

(12) Giddings, J. C. *Unified Separation Science*; John Wiley & Sons: New York, 1991; p 101.

(13) Feller, W. *An Introduction to Probability Theory and Its Applications*, 3rd ed.; Wiley: New York, 1967.

$$\theta_{\text{mig}} = \tan^{-1} \frac{Hp}{L(1-p) + L'p}$$

and when p is small, this gives approximately

$$\theta_{\text{mig}} = \frac{H}{L}p$$

or equivalently

$$p = \frac{L}{H}\theta_{\text{mig}} \quad (1)$$

This equation allows one to extract the parameter p from the experimentally measured migration angle θ_{mig} . The half-bandwidth (standard deviation) σ of this binomial distribution after N rows of obstacles is

$$\sigma^2 = \sigma_0^2 + H^2 N p(1-p) \quad (2)$$

where σ_0 is the initial half-width (standard deviation). For our choice of H , L , and L' (6, 8, and 10 μm , respectively), eqs 1 and 2 reduce to

$$p = \frac{4}{3}\theta_{\text{mig}} \quad (3)$$

and

$$\sigma^2 = \sigma_0^2 + (16 \mu\text{m}^2) N \theta_{\text{mig}} (3 - 4\theta_{\text{mig}})$$

respectively. For a given vertical distance y from the injection point, we have $N = y/[L(1-p) + L'p]$, or $N = y/[(1-p)(8 \mu\text{m}) + p(10 \mu\text{m})]$ in our case. p is small by assumption, and thus, we can substitute $y/(8 \mu\text{m})$ for N to obtain

$$\sigma^2 = \sigma_0^2 + (2 \mu\text{m}) y \theta_{\text{mig}} (3 - 4\theta_{\text{mig}}) \quad (4)$$

This equation predicts the bandwidth according to the migration angle θ_{mig} .

We now compare the theoretical predictions of bandwidths using eq 4 to the data and use the model to extrapolate the performance of larger arrays for a tilt angle of $\theta_{\text{tilt}} = 7.2^\circ$. For a speed of $\sim 1.5 \mu\text{m/s}$, the migration angles θ_{mig} and extracted ratchet probabilities p for 48.5- and 164-kb DNA were $\sim 8.3^\circ$ and $\sim 2.0^\circ$ and ~ 0.19 and ~ 0.05 , respectively. The initial bandwidth (2σ) was $\sim 53 \mu\text{m}$. At the end of the 12-mm array, the full widths of the two bands had grown to ~ 195 and $\sim 115 \mu\text{m}$, respectively. Figure 6A shows the observed and theoretical (eq 4) bandwidths as a function of position in the array, with no adjustable parameters used in the theory. Also shown for comparison are bandwidths (2σ) predicted assuming simple free diffusion of DNA in aqueous buffer, ignoring any effects of the obstacles, using diffusion constants from the literature (~ 0.64 and $\sim 0.28 \mu\text{m}^2/\text{s}$ for 48.5-

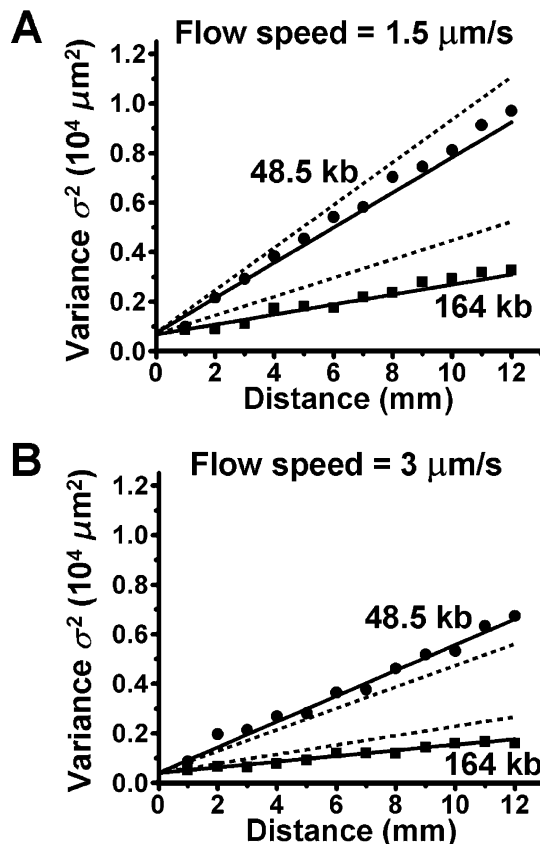


Figure 6. Measured variance (half-width squared, σ^2) of 48.5- (●) and 164-kb (■) molecules vs distance from the injection point. Flow speeds were (A) ~ 1.5 and (B) $\sim 3 \mu\text{m/s}$, respectively, at $\theta = 7.2^\circ$. Solid lines are predictions from eq 4 using measured initial widths and migration angles (Figure 4C). Dotted lines indicate band broadening expected from free diffusion alone.

and 164-kb DNA, respectively).¹⁴ Clearly, the agreement between the data and eq 4 is excellent, and free diffusion does not accurately model band broadening in our array. Similar excellent agreement between data and the ratcheting theory for a speed of $3.0 \mu\text{m/s}$ is shown in Figure 6B.

With confidence in our model of band broadening, we can extrapolate our results to predict the performance of arrays longer than the 12-mm array discussed in this paper. Because the bandwidths increase with the square root of distance and the separation of the bands increases linearly, the resolution increases as the square root of the array length. At a tilt angle of $\theta_{\text{tilt}} = 7.2^\circ$ and a DNA flow rate of $\sim 3 \mu\text{m/s}$, our 12-mm array (running time ~ 70 min) achieves a resolution of ~ 3.8 between 48.5- and 164-kb molecules (Figure 5), corresponding to the ability to resolve a 38% difference in molecular weight.¹⁵ Using the same conditions, a 37-mm-long array with a running time of 3 h 40 min should

(14) Nkodo, A. E.; Garnier, J. M.; Tinland, B.; Ren, H.; Desruisseaux, C.; McCormick, L. C.; Drouin, G.; Slater, G. W. *Electrophoresis* **2001**, *22* (12), 2424–2432.

(15) Two peaks are resolved if the resolution is larger than 1. The percentage resolution, R_p , is calculated from the resolution R_s defined in ref 12 using the equation $(1 + R_p) = (m_2/m_1)^{(1/R_s)}$, where m_2 and m_1 are molecular weights of the two peaks and $m_2 > m_1$. In our case $m_2 = 164$ kb, $m_1 = 48.5$ kb, and $R_s = 3.8$, so we get $R_p = 38\%$. To obtain $R_p = 20\%$, the resolution R_s needs to be ~ 6.7 between m_2 and m_1 , a factor of 1.76 larger than currently demonstrated ($R_s \approx 3.8$, using a 12-mm-long array). Therefore, the array should be about a factor of 1.76² longer to achieve $R_p = 20\%$.

resolve a 20% difference in the ~ 100 -kb range. Conventional PFGE typically requires ~ 10 h of running time to achieve a similar resolution in this weight range.

CONCLUSIONS

We have shown that the separation resolution and speed of microfabricated Brownian ratchet arrays for DNA separation can be improved by factors of 3 and 10, respectively, over our previous results by tilting the flow at a small angle with respect to the array. Because the amount of diffusion required for ratcheting is greatly reduced, the separation is faster, and the resolution is higher. Whereas previous experiments with no tilt required ~ 140 min of running time to resolve 48.5- from 164-kb DNA molecules (resolution = 1.4), at a flow tilt angle of 7.2° , the same resolution can be achieved in ~ 14 min, as well as a resolution of ~ 3.8 in ~ 70 min. The band broadening scales with a binomial distribution

model, which enables us to predict that the resolution improves with the square root of array length. Further, because the Brownian ratchet array does not require that the molecules be stretched, it should be useful for separating other biologically important molecules according to their diffusion coefficients.

ACKNOWLEDGMENT

This work was supported by grants from DARPA (MDA972-00-1-0031), NIH (HG01506), and the State of New Jersey (NJCST 99-100-082-2042-007). L.R.H. thanks J. O. Tegenfeldt, P. Silberzan, and members of our laboratories for discussion.

Received for review July 25, 2003. Accepted September 26, 2003.

AC0348524